TISSUE ENGINEERING: Part A
Volume 19, Numbers 19 and 20, 2013

DOI: 10.1089/ten.tea.2012.0674

Growth Factors Polymerized Within Fibrin Hydrogel Promote Amylase Production in Parotid Cells

Andrew D. McCall, BS,[1] Joel W. Nelson, BS,[1] Noel J. Leigh, BS,[1] Michael E. Duffey, PhD,[2] Pedro Lei, PhD,[3] Stelios T. Andreadis, PhD,[3–5] and Olga J. Baker, DDS, PhD[1]

Salivary gland cell differentiation has been a recurring challenge for researchers as primary salivary cells show a loss of phenotype in culture. Particularly, parotid cells show a marked decrease in amylase expression, the loss of tight junction organization and proper cell function. Previously, Matrigel has been used successfully as an extracellular matrix; however, it is not practical for *in vivo* applications as it is tumorigenic. An alternative method could rely on the use of fibrin hydrogel (FH), which has been used extensively in biomedical engineering applications ranging from cardiovascular tissue engineering to wound-healing experiments. Although several groups have examined the effects of a three-dimensional (3D) environment on salivary cell cultures, little is known about the effects of FH on salivary cell cultures. The current study developed a 3D cell culture model to support parotid gland cell differentiation using a combination of FH and growth factor-reduced Matrigel (GFR-MG). Furthermore, FH polymerized with a combination of EGF and IGF-1 induced formation of 3D spheroids capable of amylase expression and an agonist-induced increase in the intracellular Ca^{2+} concentration ($[Ca^{2+}]_i$) in salivary cells. These studies represent an initial step toward the construction of an artificial salivary gland to restore salivary gland dysfunction. This is necessary to reduce xerostomia in patients with compromised salivary function.

Introduction

Proper salivary gland function is critical for oral health. Decreased saliva production caused by Sjögren's Syndrome and head and neck γ-irradiation therapy, among other causes, leads to severe damage within the oral cavity that significantly reduces the quality of life for afflicted patients. Treatments for hyposalivation are limited to medications (e.g., the muscarinic receptor agonists, pilocarpine and cevimeline) that induce saliva secretion from residual acinar cells[1–3] and the introduction of artificial saliva.[4] Currently, there are no therapies that can provide permanent relief for afflicted patients. Therefore, alternative therapies such as the creation of an artificial salivary gland are necessary to restore salivary function.

An ideal salivary model structure would replicate the three-dimensional (3D) sphere of polarized acinar epithelial cells with tight junctions (TJ), an open lumen, and appropriate salivary function (e.g., fluid and protein secretion). This model structure can be partly generated using various gel culture systems. In a gel culture system, cells are plated on or within extracellular matrices, which allow them to form natural cell-to-cell junctions in three dimensions.[5] Two methods are commonly used to generate 3D acinar-like structures.[6] In the first method, epithelial cells are completely embedded within the extracellular matrix (ECM). In the second method (used in this study), the ECM is first cast to form a gelled bed measuring approximately 1 mm in thickness. Then, epithelial cells are seeded as a two-dimensional (2D) culture in media onto this bed and migrate from the surface to the interior of the gel, spontaneously forming 3D structures.

Previous studies have shown that submandibular gland (SMG) and parotid gland (PG) cells (from human, rat, or mouse origin) are able to grow on surfaces coated with Matrigel (MG, a solubilized basement membrane matrix extracted from murine tumor).[7] MG is rich in extracellular matrix proteins, with the major components being laminin and collagen IV. Although MG allows the formation of 3D salivary constructs from single acinar cells, it may not be suitable for clinical applications for many reasons, including the following: (1) It is originated from mouse tumor,[8] (2) The exact composition of MG is unknown leading to variability among different batches,[9] (3) MG has been found to be contaminated with a single-stranded RNA virus in some of the latest batches,[10] (4) MG, when premixed with carcinoma primary cells and injected subcutaneously into athymic mice,

[1]Department of Oral Biology, School of Dental Medicine, [2]Department of Physiology and Biophysics, School of Medicine, Departments of [3]Chemical and Biological Engineering, [4]Biomedical Engineering, School of Engineering and Applied Sciences, [5]Center of Bioinformatics and Life Sciences, University at Buffalo, The State University of New York, Buffalo, New York.

permitted tumor growth, whereas cells injected in the absence of MG did not form tumors,[11] and (5) MG promoted the formation of subcutaneous tumors in nonirradiated Severe Combined Immunodeficiency mice by a human pre-B leukemia cell line termed G2.[12] Growth Factor-Reduced Matrigel (GFR-MG) is similar to MG; however, it has been purified and characterized to a greater extent than the MG matrix. The method used to prepare this product effectively reduces the level of a variety of growth factors,[13] except for TGF-β, which may be bound to collagen IV and/or sequestered in a latent form that partitions with the major components in the purification procedure.[14] The major components, laminin, collagen IV, and entactin, are conserved during the purification process, while the level of heparan sulfate proteoglycan is reduced by 40%–50%. The purification leading to GFR-MG does not appear to reduce support for tumor growth,[15–17] thus, an alternative growth matrix must be found.

Fibrin hydrogels (FH) are water-swollen, cross-linked polymeric structures that form scaffolds and allow for 3D cell assembly. In certain cell types, FH are capable of supporting cell viability and differentiation for long periods of time.[19] This might be due to the interaction of cells with fibrin (possibly through integrin $\alpha_v\beta_3$), which may suppress caspase activation and reactive oxygen species generation.[18] Fibrin, a major protein component of blood clots, is able to form a gel at physiological temperatures. It has been used extensively in biomedical engineering applications ranging from cardiovascular tissue engineering[19,20] to wound-healing experiments (due to its biocompatibility and its ability to biodegrade *in vivo*).[21] Although several groups have studied the effects of a 3D environment on salivary cell cultures, little is known about the effects of culturing salivary cells on FH.[22–24] Moreover, the effects on cell differentiation of salivary cells grown on FH combined with GFR-MG or its components have not been previously studied. Our previous success in engineering implantable blood vessels in FH[19,20,25] led us to hypothesize that FH might be an effective growth matrix for Par-C10 and PG cells. The aim of this study was to investigate the effects of FH and GFR-MG on acinar formation and cell differentiation. These events represent an initial step for bioengineering an artificial salivary gland.

Materials and Methods

Experimental animals

Female C57BL/6 mice at 3–6 weeks of age were anesthetized via IP with 80–100 mg/kg ketamine + 5 mg/kg xylazine. Mice were euthanized by abdominal exsanguination and PGs were removed for preparation of dispersed cell aggregates. All animal usage, anesthesia, and surgery were conducted under the strict guidelines and approval of the State University of New York at Buffalo Institutional Animal Care and Use Committee.

Preparation of mouse PG single cells

Freshly dispersed cell aggregates from PGs of C57BL/6 mice were prepared as described previously.[5,26] Protocols conformed to Institutional Animal Care and Use Committee guidelines of the State University of New York at Buffalo. Briefly, mice were anesthetized and PGs removed. Glands were finely minced in a dispersion medium consisting of Dulbecco's Modified Eagle's Medium (DMEM)/Ham's F-12 (1:1) (Hyclone, Logan, UT) and 0.2 mM $CaCl_2$, 1% (wt/vol) bovine serum albumin (BSA), 50 units/mL collagenase (Worthington Biochemical, Freehold, NJ), and 400 units/mL hyaluronidase at 37°C for 30 min with aeration (95% air-5% CO_2). Cell aggregates in the dispersion medium were suspended by pipetting at 20 and 30 min. The dispersed cell aggregates were washed with an enzyme-free assay buffer (120 mM NaCl, 4 mM KCl, 1.2 mM KH_2PO_4, 1.2 mM $MgSO_4$, 1 mM $CaCl_2$, 10 mM glucose, 15 mM N-2-hydroxyethylpiperazine-N'-2-ethanesulfonic acid (HEPES), pH 7.4) containing 1% (wt/vol) BSA and filtered through a 0.22-μm nylon mesh. Cells were washed again in DMEM/Ham's F12 (1:1) containing 2.5% (v/v) fetal bovine serum (GIBCO BRL, Gaithersburg, MD) and the following supplements: 0.1 μM retinoic acid, 80 ng/mL epidermal growth factor, 2 nM triiodothyronine, 5 mM glutamine, 0.4 μg/mL hydrocortisone, 5 μg/mL insulin, 5 μg/mL transferrin, 5 ng/mL sodium selenite, and freshly added 100 μg/mL Normocin™ (InvivoGen, San Diego, CA). Cells were centrifuged at room temperature at 700 r.p.m for 5 min. Then, the supernatant was removed and the pellet was digested with 2 mL of 0.05% trypsin containing 5 mM EDTA (Invitrogen, Carlsbad, CA) for 5 min. This step was followed by neutralization with 3 mL of the DMEM-Ham's F12 (1:1) with supplements. Then, cells were consecutively filtered through 0.7- and 0.4-μm nylon meshes, and approximately 2,000 cells/well were plated on top of different extracellular matrices (prepared as described below) as a 2D culture and incubated for 3 days at 37°C with 95% air and 5% CO_2. Any cells remaining after plating were centrifuged at 3,000 r.p.m. for 30 s and used as freshly isolated positive controls for Western blots.

Preparation of Par-C10 single cells

The Par-C10 cell line was derived from freshly isolated rat parotid gland acinar cells by transformation with simian virus 40 and exhibits many characteristics of freshly isolated acinar cells.[27,28] Par-C10 cells (1×10^4 cells/well; passage 40–60) in a 10% (vol/vol) dilution were prepared from a confluent flask using DMEM/Ham's F12 (1:1) with supplements, as indicated in section 'Preparation of mouse PG single cells'. Cells were then filtered through a 0.4-μm nylon mesh, and approximately 2,000 cells/well were plated on top of different extracellular matrices (prepared as described below) as a 2D culture and incubated for 3 days at 37°C with 95% air and 5% CO_2.

Preparation of GFR-MG

One hundred microliters of GFR-MG (8 mg/mL /well; 2:1 GFR-MG: DMEM/Ham's F12 (1:1) serum-free medium; Becton Dickinson Labware, Franklin Lakes, NJ) was allowed to solidify in a 37°C incubator for 1 h in eight-well chambers mounted on #1 German borosilicate coverglasses (Nalge Nunc International Corporation, Naperville, IL). Cells were plated on the GFR-MG in DMEM/Ham's F12 (1:1) medium with supplements, overnight, as indicated in section 'Preparation of mouse PG single cells'. Cells were maintained in the serum-free medium for an additional 2 days. However, 2.5% FBS was used in cells grown for immunofluorescence studies (to improve adherence).

Preparation of FH

Plasma-derived bovine thrombin (2.5 U/mL) was added to fibrinogen (2.5 mg/mL) in Tris-buffered saline (TBS) with $CaCl_2$ (2.5 mM) and Epsilon-aminocaproic acid (EACA, 2 mg/mL) (as described in previous studies).[29] One hundred microliters of this mixture (FH) was allowed to solidify in a 37°C incubator overnight in eight-well chambers.

Preparation of FH+ GFR-MG

A 50 μL mixture of fibrinogen (5.0 mg/mL), thrombin (5.0 U/mL), and EACA (4 mg/mL) in TBS with $CaCl_2$ (2.5 mM) was combined with 50 μL of GFR-MG (5.3 mg/mL) (FH+GFR-MG). The mixture was placed in eight-well chambers as described above.

Preparation of FH with different doses of EGF and IGF-1

Different doses of EGF and IGF-1 [as indicated in the figure legends (Fig. 5A, B)] were added to 100 μL of the FH mixture. The mixture was placed in eight-well chambers and allowed to solidify as described above for FH.

Intracellular-free Ca^{2+} concentration measurements

The intracellular-free Ca^{2+} concentration ($[Ca^{2+}]_i$) was quantified in single Par-C10 and PG cells grown on all growth matrices and preloaded with Fura-2, a Ca^{2+}-sensitive fluorescent dye, using a MetaFluor dual wave length fluorescence imaging system (Molecular Devices, Sunnyvale, CA) as described previously.[30] For Fura-2 preloading, Par-C10 and PG cells on eight-well glass coverslips were incubated with an enzyme-free assay buffer (as described in 2.2) containing 4 μM fura-2-acetoxymethylester (fura-2-AM; Molecular Probes, Eugene, OR) for 20 min at 37°C, washed with the assay buffer, and further incubated for 20 min in Ca^{2+}-containing DMEM/Ham's F12 (1:1) with supplements at 37°C in a 5% CO_2 atmosphere. The cells were positioned on the stage of a fluorescence microscope and stimulated with 100 μM carbachol (Cch; Sigma, St. Louis, MO) at room temperature. Fura-2 AM fluorescence images at 340 nm and 380 nm excitation wavelengths were captured at 510 nm wavelength with a Hamamatsu C2400 camera. Average fluorescence ratio values (340/380 ratio) from single structures were determined.

Confocal microscopy

Par-C10 and PG cells were fixed in 4% paraformaldehyde for 20 min at room temperature, incubated with 0.1% Triton X-100 in phosphate-buffered saline (PBS) for 5 min and washed with PBS. Cells were then incubated with 5% goat serum containing 10 μM digitonin for 2 h at room temperature and washed three times with PBS. Cells were incubated overnight at 4°C with rabbit anti-ZO-1 (1:400 dilution in 5% goat serum containing 10 μM digitonin; Invitrogen). The next day, acinar spheres were warmed to room temperature for 20 min and washed three times for 5 min with PBS. Spheres were incubated for 1 h with Alexa Fluor 488-conjugated goat anti-rabbit (1:500 dilution in 5% goat serum containing 10 μM digitonin; Sigma) and washed three times with PBS. Spheres were stained for 15 min with Alexa Fluor 568-conjugated phalloidin F-actin stain (1:400 dilution in PBS; Sigma) and for 5 min with a Hoechst nuclear stain (1:20,000 dilution in PBS; Sigma). Images were obtained using a Carl Zeiss 510 confocal microscope.

Western blot analysis

Single PG cells grown on GFR-MG, FH, FH+GFR-MG, and FH+EGF and IGF-1, as well as freshly isolated PG cells (positive control), were lysed in 200 μL of 2×Laemmli buffer with 10 mM dithiotreitol and lysates were sonicated for 30 s with a Fisher Scientific Sonic Dismembrator (model FB-120, microtip; output level 5; duty cycle 50%) and boiled for 3 min. The lysates were subjected to 4%–15% (wt/vol) SDS-PAGE (Bio-Rad, Hercules, CA) on mini gels and transferred to nitrocellulose membranes. Membranes were blocked for 1 h with 5% (wt/vol) nonfat dry milk in TBS [0.137 M NaCl, 0.025 M Tris (hydroxymethyl)-aminomethane, pH 7.4] containing 0.1% (vol/vol) Tween-20 (TBST) and immunoblotted overnight at 4°C with a rabbit anti-α-Amylase (D55h10) primary antibody [1:500 dilution in TBST containing 3% (wt/vol) BSA; Cell Signaling Technology, Beverly, MA]. After incubation with the primary antibody, membranes were washed three times for 15 min each with TBST and incubated with a peroxidase-linked goat anti-rabbit IgG antibody [1:5,000 dilution in TBST containing 5% (wt/vol) nonfat dry milk; Cell Signaling Technology], at room temperature for 1 h. The membranes were washed three times for 15 min each with TBST and treated with a femto chemiluminescence detection reagent (Thermo Scientific, Rockford, IL). The protein bands were visualized using a Bio-Rad ChemiDoc™ MP imager and quantification of the bands was performed using Image Lab 4.1 software (Bio-Rad). For signal normalization, membranes were treated with a stripping buffer [0.2 M glycine, 1% (v/v) Tween-20, and 3.5 mM sodium dodecyl sulfate pH 2.2] and reprobed with a rabbit anti-β-Tubulin antibody (1:800 dilution; Abcam) followed by incubation with the peroxidase-linked goat anti-rabbit IgG antibody as described above. α-Amylase (D55h10) was expressed as a ratio of normalized values of the band intensities of α-Amylase (D55h10) to β-Tubulin.

Statistical analysis

Data are means ± SEM of results from three or more experiments. p values < 0.05 calculated from one-way ANOVA represent significant differences.

Results

Growth of Par-C10 and PG single cells on GFR-MG

In an effort to find a suitable matrix to grow primary cells, we used GFR-MG to grow mouse PG single cells following optimization of matrix and culture conditions using Par-C10 cells. As shown in Figure 1A–H Par-C10 and PG single cells formed 3D acinar structures when grown on GFR-MG, after 3 days. Acinar structures were defined as spheres with hollow lumens, determined by the presence of apical expression of the TJ protein zonula occludens-1 (ZO-1, Fig. 1A, E) and a F-actin ring at the apical surface (Fig. 1B, F). Furthermore, both Par-C10 and PG single cells displayed increases in $[Ca^{2+}]_i$ (seen as increases in the 340/380 ratio) in response to

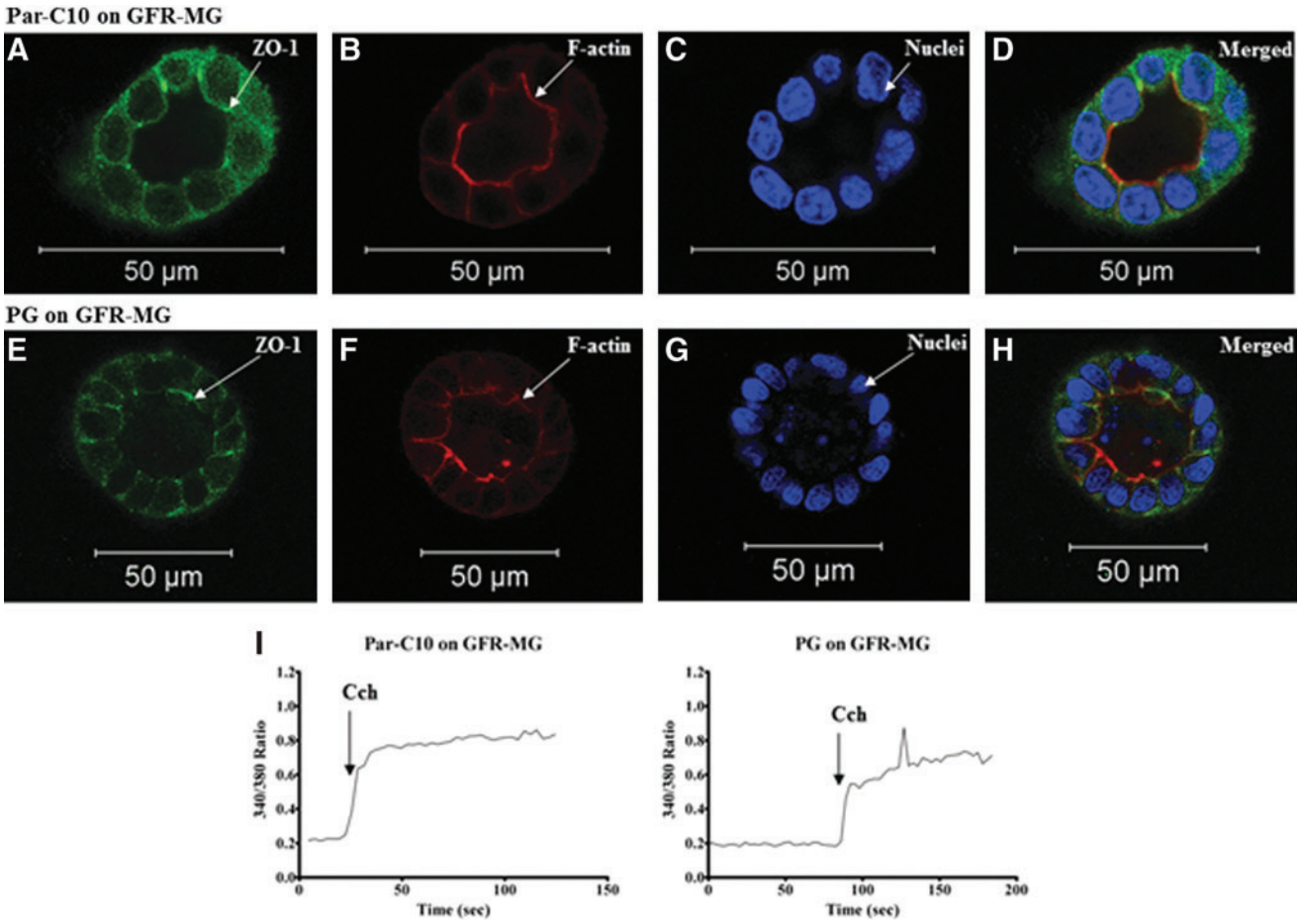

FIG. 1. The effect of growth factor-reduced Matrigel (GFR-MG) on Par-C10 and parotid gland (PG) single cells. Single cells grown on GFR-MG for 3 days were analyzed using immunofluorescence microscopy using rabbit anti-ZO-1 **(A, D, E, H;** green**)**, phalloidin staining **(B, D, F, H;** red**)**, and Hoechst nuclear stain **(C, D, G, H;** blue**)**. The *xy* cross-section images were obtained using a Carl Zeiss 510 confocal microscope. All scale bars represent 50 μm. Cells were stimulated with Carbachol (100 μM) and changes in the Fura-2 Fluorescence ratio recorded at 340 and 380 nm were monitored **(I)** as described in Materials and Methods. Results from a representative of three experiments are shown. Color images available online at www.liebertpub.com/tea

the salivary muscarinic receptor agonist Cch, indicative of secretory function (Fig. 1I).

Growth of Par-C10 and PG single cells on FH

Par-C10 cells usually formed monolayers when grown on FH, after 3 days. As shown in Figure 2A–D, we observed tubular-like structures with the absence of lumens as well as randomly dispersed flat cell islands; few of these structures expressed ZO-1, but did not display a 3D organized round structure and consequently lacked an F-actin ring. As shown in Figure 2E–H, PG cells either failed to grow or sparsely formed 3D structures lacking lumens, referred to as spheroids (i.e., they lacked an F-actin ring, few of them faintly expressed ZO-1, and the TJs were not organized to an apical surface). In addition, some PG cells plated on FH had characteristics of blebbing, indicating cell death. Taken together, these results suggest that FH alone is not suitable to sustain cell growth and differentiation. However, both Par-C10 and PG single cells displayed increases in $[Ca^{2+}]_i$ in response to Cch, again indicating their ability to respond to secretory agonists (Fig. 2I).

Growth of Par-C10 and PG single cells on FH+GFR-MG

Since FH alone was not suitable for sustained differentiated growth in Par-C10 and PG, we decided to determine if a combination of MG and FH would enhance acinar formation and cell differentiation. As shown in Figure 3A–D, single Par-C10 cells plated on combinations of GFR-MG and FH for 3 days formed flat monolayers that contoured to the ECM (i.e., with concave and convex areas). Surprisingly, we did not see recovery of luminal structures and ZO-1 staining in Par-C10 monolayers grown on FH+GFR-MG. PG cells plated on FH and GFR-MG combinations formed spheroids that lacked an F-actin ring and displayed sporadic expression of ZO-1 (Fig. 3E–H). Furthermore, both Par-C10 and PG cells were able to respond to Cch (Fig. 3I).

Par-C10 and PG single cells grown on FH+EGF+IGF-1

To determine which components of GFR-MG may play a role in acinar formation and differentiation, we added growth factors present in the GFR-MG into the FH during

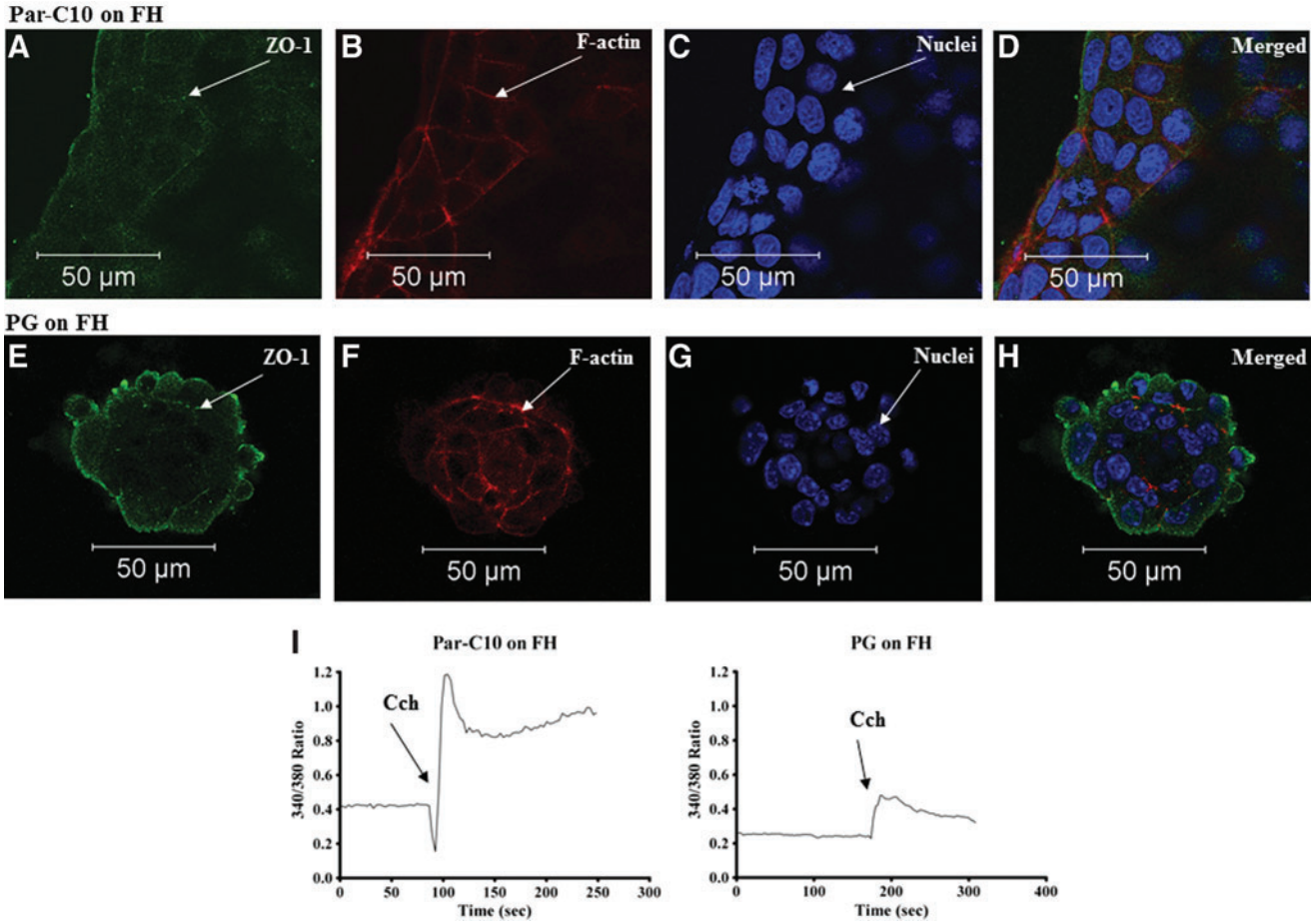

FIG. 2. The effect of Fibrin Hydrogels (FH) on Par-C10 and PG single cells. Single cells grown on FH for 3 days were analyzed using immunofluorescence microscopy using rabbit anti-ZO-1 **(A, D, E, H;** green**)**, phalloidin staining **(B, D, F, H;** red**)**, and Hoechst nuclear stain **(C, D, G, H;** blue**)**. The *xy* cross-section images were obtained using a Carl Zeiss 510 confocal microscope. All scale bars represent 50 μm. Cells were stimulated with Carbachol (100 μM) and changes in the Fura-2 Fluorescence ratio recorded at 340 and 380 nm were monitored **(I)** as described in Materials and Methods. Results from a representative of three experiments are shown. Color images available online at www.liebertpub.com/tea

polymerization at a significantly increased concentration as compared with GFR-MG [i.e., EGF (50 ng/mL) and IGF-1 (50 ng/mL) in combination]. As shown in Figure 4A–D, growth of Par-C10 cells plated on FH + EGF + IGF-1 was not significantly different from the growth of Par-C10 cells plated on FH alone in terms of acinar formation, as they both formed monolayers with low ZO-1 expression (Fig. 2A–D). Similarly, the growth of PG cells plated on FH + EGF + IGF-1 (Fig. 4E–H) was not significantly different from the growth of PG cells plated on FH (Fig. 2E–H) as they are both spheroids with low ZO-1 expression and lack a defined acinar lumen. Both Par-C10 and PG were viable as they maintained the ability to respond to Cch (Fig. 4I).

Dose responses of PG single cells grown on FH+ EGF+ IGF-1

Because EGF and IGF-1 are known to enhance amylase expression, we decided to test for enhanced differentiation of PG cells (as indicated by increase of amylase expression) grown on FH + EGF + IGF-1. To do this, we performed a dose–response study by polymerizing within FH, a constant dose of EGF (50 ng/mL) with variable concentrations of IGF-1 (0–50 ng/mL) or a constant dose of IGF-1 (50 ng/mL) with variable concentrations of EGF (0–50 ng/mL). As shown in Figure 5A, EGF (50 ng/mL) + IGF-1 (0–50 ng/mL) were able to stimulate amylase expression in mouse PG in a dose-dependent manner. Statistical analyses revealed that amylase expression of PG cells grown at the peak of the dose–response curve [EGF (50 ng/mL) + IGF-1 (50 ng/mL)] was significant as compared to cells plated on GFR-MG, but not significantly different from cells grown on FH alone and GFR-MG + FH. These results indicate that an increased concentration of growth factors within FH enhances amylase expression. Similarly, when cells were grown with a constant concentration of IGF-1 (50 ng/mL) and variable EGF (0–50 ng/mL), amylase expression was also increased in a dose-dependent manner (Fig. 5B), with significant differences present only between cells grown on FH with IGF-1 (50 ng/mL) and EGF (20 ng/mL) as compared to cells grown on GFR-MG, FH, and GFR-MG + FH. For simplicity, select significant differences were not indicated on Figure 5B, including significance with cells grown on EGF (10, 40, and 50 ng/mL) with IGF-1 (50 ng/mL) as compared to GFR-MG and

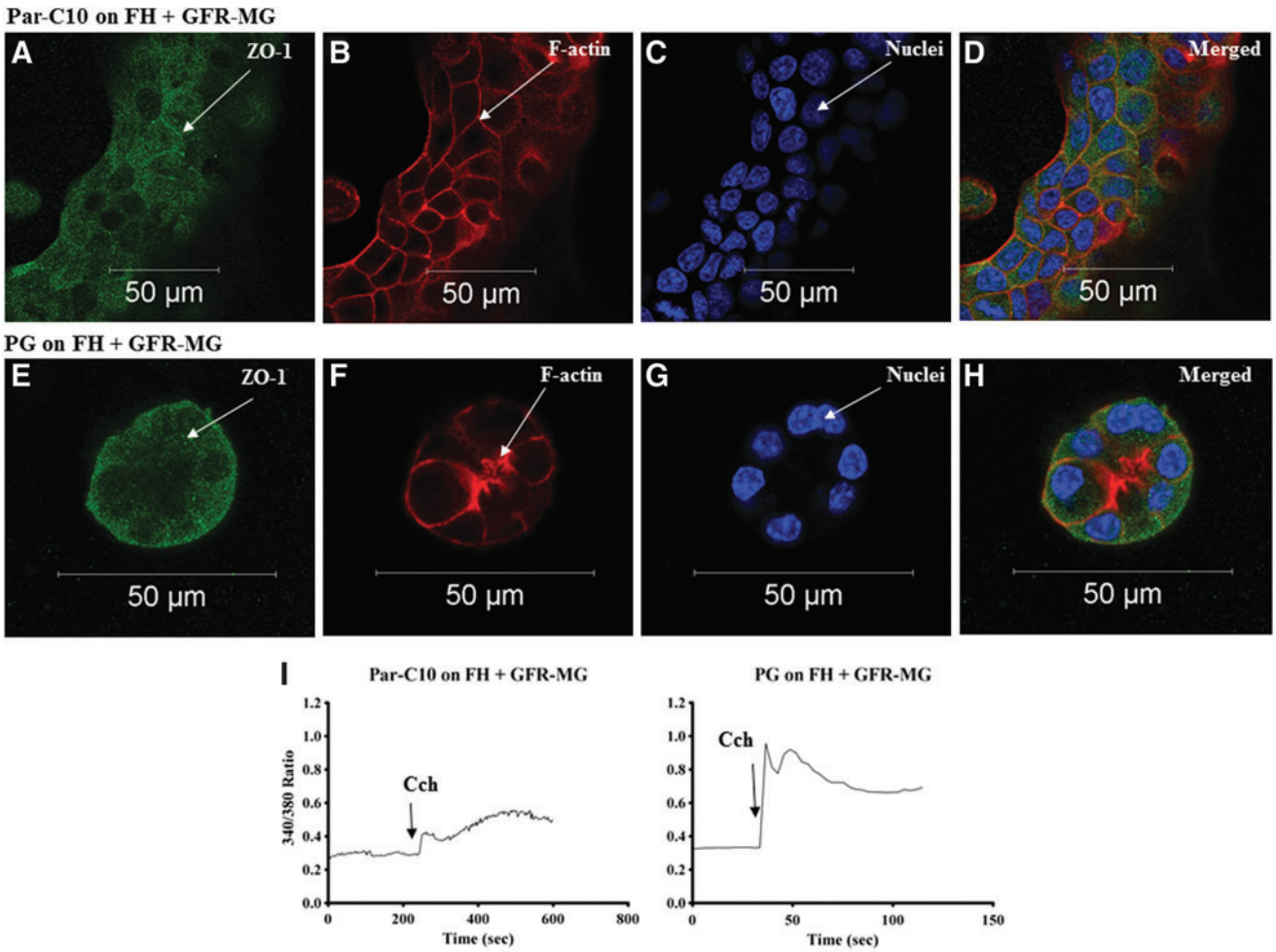

FIG. 3. The effect of FH + GFR-MG on Par-C10 and PG single cells. Single cells grown on FH + GFR-MG for 3 days were analyzed using immunofluorescence microscopy using rabbit anti-ZO-1 **(A, D, E, H;** green**)**, phalloidin staining **(B, D, F, H;** red**)**, and Hoechst nuclear stain **(C, D, G, H;** blue**)**. The *xy* cross-section images were obtained using a Carl Zeiss 510 confocal microscope. All scale bars represent 50 µm. Cells were stimulated with Carbachol (100 µM) and changes in the Fura-2 Fluorescence ratio recorded at 340 and 380 nm were monitored **(I)** as described in Materials and Methods. Results from a representative of three experiments are shown. Color images available online at www.liebertpub.com/tea

FH + GFR-MG in combination. Nevertheless, these results indicate that combinations of EGF and IGF-1 polymerized within FH induced maximal amylase expression.

Discussion

Our previous study demonstrated that a rat parotid gland cell line (Par-C10) could be grown on GFR-MG to form structures that closely resembled the 3D *in vivo* environment (acinar structures capable of developing TJs).[5] Here we used primary PG single cells grown on GFR-MG and demonstrated that PG cells were able to grow in clusters and form lumens (Fig. 1E-H). Although Matrigel has been used previously to grow salivary cells,[22–24,31–34] it has been a challenge to maintain cell differentiation, determined by normal cellular function and maintenance of amylase expression, with time in culture. In this study, both single Par-C10 (Fig. 1A–D) and PG (Fig. 1E–H) were able to form acinar structures on GFR-MG, indicating an intrinsic ability of components within GFR-MG to enhance differentiation.

Given that GFR-MG is tumorogenic and immunogenic,[15–17] an alternative material that can be clinically applied to patients should be developed. FH have been used as scaffolds for stem cells and primary cells to grow a variety of tissues, including adipose tissue, bone, cardiac tissue, cartilage, liver, nervous tissue, ocular tissue, skin, tendons, and ligaments.[35] Furthermore, FH are made up of physiological components,[20] which make FH adaptable scaffolds with a great potential for tissue-engineering applications. However, no previous studies have explored the possibility of growing salivary gland cells on FH. Here we found that Par-C10 cells were able to grow as highly proliferative monolayers on FH (Fig. 2A–D). This is likely due to the immortalization process used to generate the Par-C10 cell line,[36] allowing them to survive for longer periods of time as compared to freshly isolated PG cells. However, because PG cells require growth factors for continuous survival,[37] they grew scarcely in spheroids displaying a low level of organization when plated on FH (Fig. 2E–H). Therefore, we evaluated the feasibility of using FH in combination with GFR-MG (which naturally

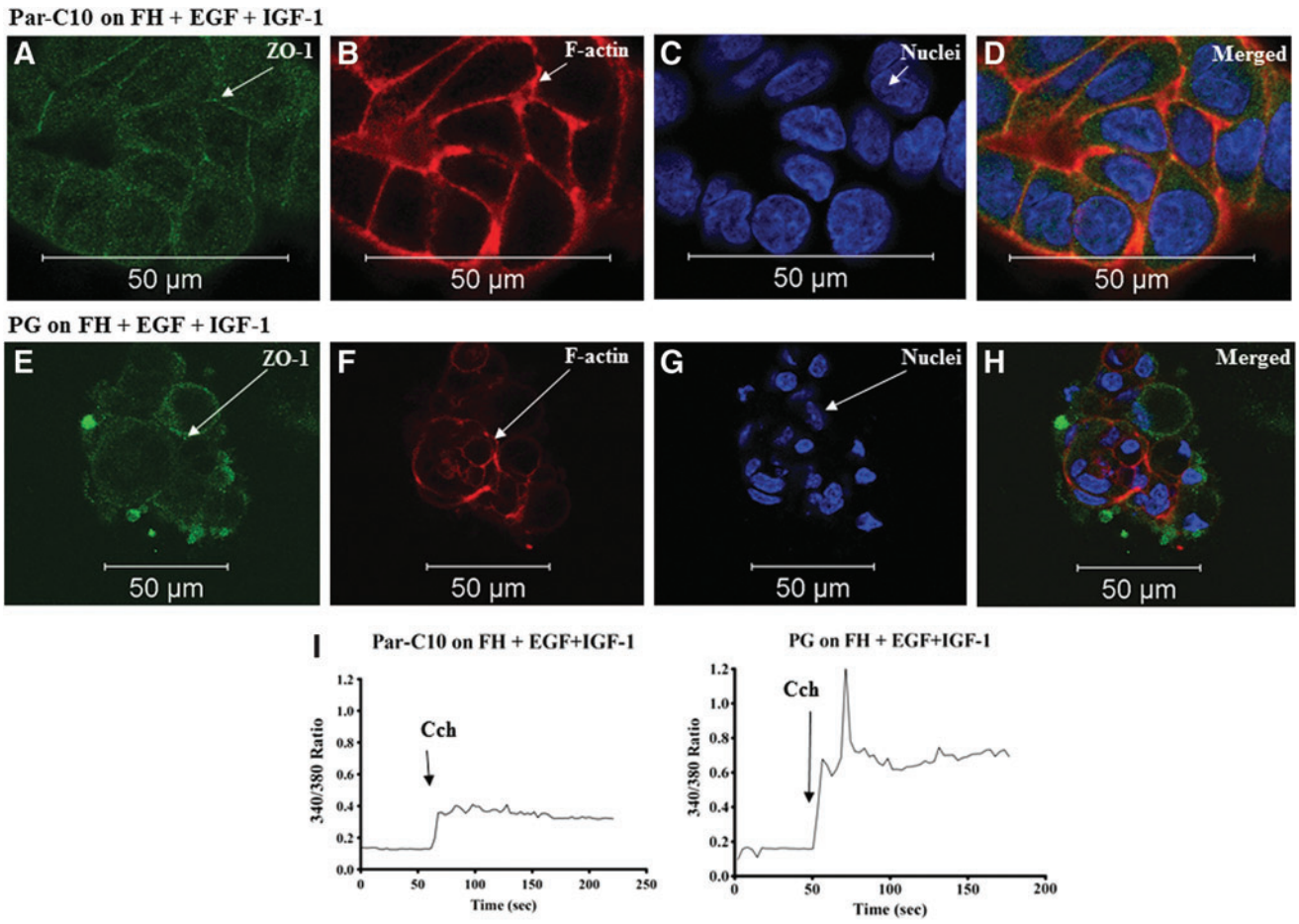

FIG. 4. The effect of FH + EGF + IGF-1 on Par-C10 and PG single cells. Single cells grown on FH + EGF + IGF-1 for 3 days were analyzed using immunofluorescence microscopy using rabbit anti-ZO-1 **(A, D, E, H;** green**)**, phalloidin staining **(B, D, F, H;** red**)**, and Hoechst nuclear stain **(C, D, G, H;** blue**)**. The *xy* cross-section images were obtained using a Carl Zeiss 510 confocal microscope. All scale bars represent 50 μm. Cells were stimulated with Carbachol (100 μM) and changes in the Fura-2 Fluorescence ratio recorded at 340 and 380 nm were monitored **(I)** as described in Materials and Methods. Results from a representative of three experiments are shown. Color images available online at www.liebertpub.com/tea

contains growth factors) to promote the formation of a differentiated acinar structure in primary PG single cells. While this combination is still tumorogenic, we thought it would provide us enough information to discover if growth factors present in the GFR-MG, in combination with FH, could enhance acinar differentiation (which could be used to later create a safe scaffold for clinical application).

On a combination of FH and GFR-MG, Par-C10 cells grew mostly as monolayers similar to FH alone (Fig. 3A–D). These results indicate that critical concentrations of components present in GFR-MG are necessary to achieve optimal growth and differentiation. PG cells grown on FH + GFR-MG grew as spheroids with no lumens and sparsely expressed ZO-1 (Fig. 3E–H) similar to PGs grown on FH alone (Fig. 2). These results further indicate that optimal concentrations of GFR-MG components are necessary to enhance acinar cell growth and differentiation.

Viable and actively growing primary salivary acinar cells can be maintained for about 3 weeks in culture.[38,39] Dedifferentiation (as indicated by decreased amylase expression and cell polarity) is the biggest challenge that must be overcome for the creation of a functional artificial salivary gland.[40] GFR-MG contains six growth factors, four of which have been demonstrated to induce no increase in the amylase promoter activity (i.e., bFGF at 0.1 ng/mL, PDGF at <5 ng/mL, NGF at <0.2 ng/mL, and TGFβ at 1.7 ng/mL).[31,34] Of the two remaining growth factors, one (EGF at <0.5 ng/mL) was shown to increase the acinar cell-specific amylase promoter activity.[31,34] The other (IGF-1 at 5 ng/mL) was not tested in the cited studies (for reasons not stated by the researchers). However, results of a subsequent study involving mice undergoing radiation treatment (which typically results in salivary gland dysfunction) indicate IGF-1 restores cell proliferation and amylase secretion.[41] Furthermore, both growth factors synergistically suppress apoptosis in salivary acinar cells.[37] Given these studies and because of the presence of EGF and IGF-1 in GFR-MG, we decided to test whether these growth factors polymerized within FH were able to show similar effects as those observed in Par-C10 and PGs when grown on the combined matrix (i.e., FH + GFR-MG). Par-C10 cells grew as monolayers when plated on FH with EGF and IGF-1 (Fig. 4A–D) and PG cells were unable to form differentiated structures (Fig. 4E–H); these results were very similar to the ones

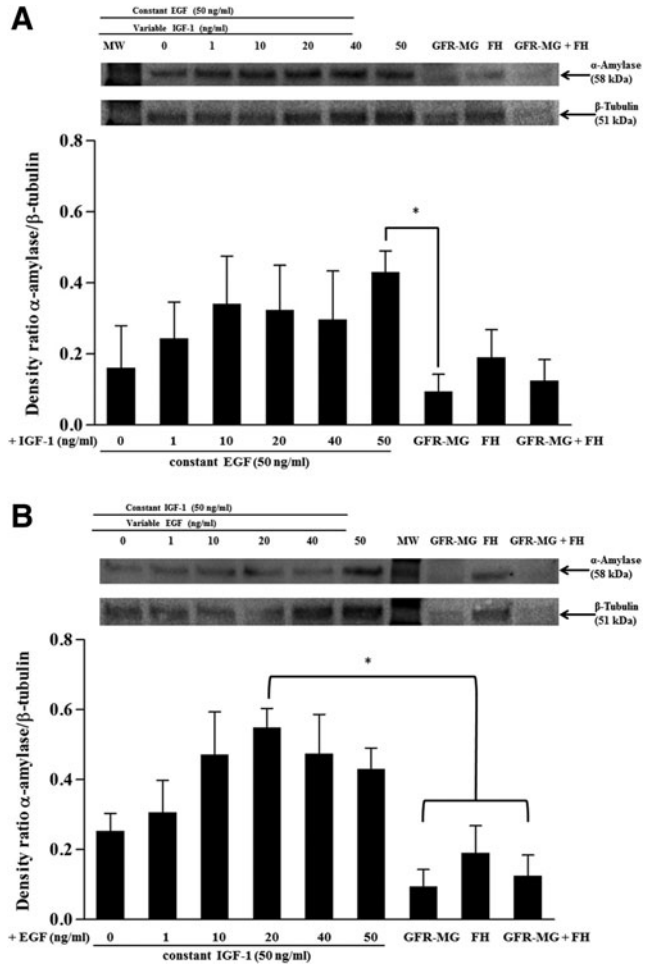

FIG. 5. α-Amylase expression in single PG cells grown on FH polymerized with growth factors. Single PG cells were grown on FH polymerized with **(A)** a constant EGF concentration (50 ng/mL) and variable IGF-1 concentrations (0–50 ng/mL), or **(B)** a constant IGF-1 concentration (50 ng/mL) and variable EGF concentrations (0–50 ng/mL). After 3 days, cells were lysed with the Laemmli buffer. Protein extracts were subjected to SDS-PAGE and immunoblotted for α-Amylase and β-Tubulin. Top: results from a representative experiment are shown ($n = 3$). Bottom: ratio of normalized values of the band intensities of α-Amylase (D55h10) to β-Tubulin using Image Lab 4.1 software. Data are expressed as the means ± SEM of results from three or more experiments, where $^*p < 0.05$ indicates significant differences from control cells.

observed on FH alone. Unexpectedly, high concentrations of the two growth factors could not coax the cells to form luminal structures similar to the ones observed on GFR-MG.

Given that amylase expression is a crucial factor for parotid cell differentiation,[42,43] we also studied the expression pattern of this protein in PG cells grown on FH with EGF and IGF-1. Previous research has shown that SMG and PG primary cells lose amylase expression after 24 h in culture when grown on plastic.[44,45] In this study, PG single cells exhibited a low amylase expression when grown on GFR-MG and FH, alone and in combination, as compared to cells cultured with FH supplemented with growth factors (Fig. 5A, B). These results indicate that the growth factors present in GFR-MG were not enough to maintain cell differentiation in these cultures. Interestingly, PG cells grown on FH supplemented with EGF and IGF-1 were able to increase amylase expression as compared to PG cells grown on GFR-MG and FH, alone and in combination (Fig. 5A, B). We also determined that the optimal concentration to grow primary PG cells was with IGF-1 (50 ng/mL) combined with EGF (20 ng/mL) as compared with FH in the absence of growth factors. These results suggest that polymerization of EGF and IGF-1 within FH allows for presentation of the growth factors along the entire basal surface of the spheroid or acinar structure and may trigger signaling mechanisms that increase amylase expression in parotid cells.

Growth factors and their receptors are known to activate MAPK/ERK pathways[46] required for salivary gland growth and differentiation.[34,47] In particular, IGF-1 binds to IGF-1R to induce differentiation in adipocytes, myoblasts, osteoblasts, neurons, and hematopoietic cells.[48] Following stimulation with IGFs, the SH2-containing adaptor protein Shc is recruited to phosphorylated tyrosine residue (Tyr950) in the juxtamembrane region of the IGF-1R. This, in turn, transduces differentiation signals through the Grb2/Ras/Raf/MEK/EKR1/2 pathway.[49] The IGF-1R is also involved in suppression of apoptosis (through the PI3K pathway, as well as by activation of ERKs and p38 MAPK).[50] EGF has been shown to regulate salivary gland morphogenesis, increase integrin expression, and alter salivary cell interactions with the ECM.[51–53] EGF also binds to the EGFR to phosphorylate MAPK pathways (including the Ras/Raf/MEK/ERK1/2 phosphorylation cascade).[52] The phosphorylated EGFR may also activate PLC (which in turn activates PKC and MAPK).[31,54] Interactions between the EGFR and IGF-1R occur in the following ways: (1) through direct contact between these two growth factor receptors, (2) through interaction partners (e.g., GPCR and their signaling molecules), and (3) in competition with one another, by restricting and granting growth factor access (each to the other).[55] Based on the information stated above, it is clear that EGF and IGF-1 are very important to maintain differentiation in PG primary cells. Moreover, future studies are necessary to understand how these signaling mechanisms regulate amylase expression. Because PG primary cells in these studies did not achieve full differentiation (besides the increased amylase expression), we believe other growth factors or ECM components may play an important role in guiding single salivary epithelial cells to form complex phenotypes; for instance, looking at which factors are upregulated during salivary gland development[56] may provide a hint to discover which factors contribute to the creation of a functional gland.

Activation of G protein-coupled muscarinic receptors in Par-C10 and PG cells stimulates phospholipase C to mediate inositol 1,4,5-trisphosphate-dependent increases in $[Ca^{2+}]_i$ due to Ca^{2+} release from intracellular stores and Ca^{2+} entry via activation of store-operated Ca^{2+} channels.[28,57,58] Therefore, to ensure cell viability and appropriate functionality, we determined whether Par-C10 and PG single cells were able to elicit increases in $[Ca^{2+}]_i$ in response to relevant salivary secretory agonists such as Cch when grown on the different extracellular matrices used in this study. As shown in Figure 1–4I, the salivary secretory agonist Cch induced increases

in $[Ca^{2+}]_i$ in Par-C10 and PG single cells grown on all growth matrices. These results indicate that agonist-induced intracellular signaling in the cell systems used here (Par-C10 and PG) remain intact regardless of the composition of the extracellular matrices.

Cell lines might not completely reflect how primary cells behave both *in vitro* and *in vivo,* and it would be difficult to measure the effectiveness of growth matrices on cell lines. Therefore, primary cells should be the main source for studies in tissue engineering. A beautiful *ex vivo* organ culture model using an embryonic bud of a mouse SMG shows that cells in culture have an innate ability to branch and display polarity similar to native tissue.[59] However, no studies have looked at whether this model is suitable for measuring saliva secretion in response to secretory agonists. Because salivary gland dysfunction afflicts well-developed glands, the *ex vivo* organ culture is not applicable to grow a salivary gland for clinical purposes. Therefore, we have to find the elements within the ECM or within single cells that cause cell survival, polarity, differentiation, and proper function. From our experiments, it is clear that GFR-MG contains these elements and that they are present at the sufficient concentrations, which appear to be required for acinar formation, but not complete cell differentiation (i.e., amylase expression). Here we have developed a new method to increase amylase expression in primary PGs by polymerization of growth factors within FH. This is the first study that delivers growth factors in single acinar cells to sustain and improve amylase production. It is likely that incorporation of other growth factors (e.g., FGF and NGFa), as well as ECM components (e.g., laminin and collagen IV), into FH will improve this model as they might influence cell differentiation, migration, adhesion as well as phenotypes and survival. In addition, incorporation of growth factors and ECM components could enhance the progenitor cell population to maintain cell growth, which has been shown to be relatively low in early culture stages.[60]

Conclusion

We reported that Par-C10 and PG single cells are capable of forming 3D structures with lumens and TJs when grown on the GFR-MG. However, both Par-C10 and PG cells grown on FH failed to completely develop, indicating that components present on GFR-MG may induce a degree of differentiation in parotid single cells. Following these studies, we decided to combine GFR-MG with FH in an attempt to recover acinar formation. Surprisingly, this combination did not result in a recovery of acinar formation for either Par-C10 or PG cells, indicating that the acinar-inducing components of GFR-MG require a critical concentration to be functional. To determine what components of GFR-MG may be necessary for differentiation, we decided to incorporate two growth factors that enhance cell survival and differentiation in salivary cells (e.g., EGF and IGF-1) into FH. While these factors were not enough to induce acinar formation, they were able to induce amylase expression in PG primary cells. Addition of these and other growth factors (e.g., FGF and NGFa) together with ECM proteins (e.g., laminin and collagen IV) may better mimic the dynamic and physiological microenvironment necessary to induce acinar formation.

Acknowledgments

The authors would like to acknowledge Dr. Wade J. Sigurdson, Director of the Confocal Microscopy and 3D Imaging Core Facility of the School of Medicine and Biomedical Sciences, the State University of New York at Buffalo (UB), for assistance in imaging of specimens. This work was supported by the NIH-NIDCR grants R21-DE19721-01A1; 1R01DE021697-01A1 (to OB); 1R01DE022971-01 (to OB and SA).

Disclosure Statement

No competing financial interests exist.

References

1. Fox, P.C., and Mandel, I.D. Effects of pilocarpine on salivary flow in patients with Sjogren's syndrome. Oral Surg Oral Med Oral Pathol **74,** 315, 1992.
2. Rhodus, N.L., and Schuh, M.J. Effects of pilocarpine on salivary flow in patients with Sjogren's syndrome. Oral Surg Oral Med Oral Pathol **72,** 545, 1991.
3. Braga, M.A., Tarzia, O., Bergamaschi, C.C., Santos, F.A., Andrade, E.D., and Groppo, F.C. Comparison of the effects of pilocarpine and cevimeline on salivary flow. Int J Dent Hyg **7,** 126, 2009.
4. Silvestre, F.J., Minguez, M.P., and Sune-Negre, J.M. Clinical evaluation of a new artificial saliva in spray form for patients with dry mouth. Med Oral Patol Oral Cir Bucal **14,** E8, 2009.
5. Baker, O.J., Schulz, D.J., Camden, J.M., Liao, Z., Peterson, T.S., Seye, C.I., Petris, M.J., and Weisman, G.A. Rat parotid gland cell differentiation in three-dimensional culture. Tissue Eng Part C Methods **16,** 1135, 2010.
6. Debnath, J., and Brugge, J.S. Modelling glandular epithelial cancers in three-dimensional cultures. Nat Rev Cancer **5,** 675, 2005.
7. Kleinman, H.K., McGarvey, M.L., Hassell, J.R., Star, V.L., Cannon, F.B., Laurie, G.W., and Martin, G.R. Basement membrane complexes with biological activity. Biochemistry **25,** 312, 1986.
8. Orkin, R.W., Gehron, P., McGoodwin, E.B., Martin, G.R., Valentine, T., and Swarm, R. A murine tumor producing a matrix of basement membrane. J Exp Med **145,** 204, 1977.
9. Janiak, M., Hashmi, H.R., and Janowska-Wieczorek, A. Use of the Matrigel-based assay to measure the invasiveness of leukemic cells. Exp Hematol **22,** 559, 1994.
10. Nagaoka, M., Si-Tayeb, K., Akaike, T., and Duncan, S.A. Culture of human pluripotent stem cells using completely defined conditions on a recombinant E-cadherin substratum. BMC Dev Biol **10,** 60, 2010.
11. Fridman, R., Kibbey, M.C., Royce, L.S., Zain, M., Sweeney, M., Jicha, D.L., Yannelli, J.R., Martin, G.R., and Kleinman, H.K. Enhanced tumor growth of both primary and established human and murine tumor cells in athymic mice after coinjection with Matrigel. J Natl Cancer Inst **83,** 769, 1991.
12. Ishii, E., Greaves, A., Grunberger, T., Freedman, M.H., and Letarte, M. Tumor formation by a human pre-B leukemia cell line in scid mice is enhanced by matrigel and is associated with induction of CD10 expression. Leukemia **9,** 175, 1995.
13. Taub, M., Wang, Y., Szczesny, T.M., and Kleinman, H.K. Epidermal growth factor or transforming growth factor alpha is required for kidney tubulogenesis in matrigel cultures

in serum-free medium. Proc Natl Acad Sci U S A **87,** 4002, 1990.
14. Paralkar, V.M., Vukicevic, S., and Reddi, A.H. Transforming growth factor beta type 1 binds to collagen IV of basement membrane matrix: implications for development. Dev Biol **143,** 303, 1991.
15. Wang, S., Nagrath, D., Chen, P.C., Berthiaume, F., and Yarmush, M.L. Three-dimensional primary hepatocyte culture in synthetic self-assembling peptide hydrogel. Tissue Eng Part A **14,** 227, 2008.
16. Lee, J., Cuddihy, M.J., and Kotov, N.A. Three-dimensional cell culture matrices: state of the art. Tissue Eng Part B Rev **14,** 61, 2008.
17. Polykandriotis, E., Arkudas, A., Horch, R.E., and Kneser, U. To matrigel or not to matrigel. Am J Pathol **172,** 1441; author reply 1441, 2008.
18. Kongkaneramit, L., Sarisuta, N., Azad, N., Lu, Y., Iyer, A.K., Wang, L., and Rojanasakul, Y. Dependence of reactive oxygen species and FLICE inhibitory protein on lipofectamine-induced apoptosis in human lung epithelial cells. J Pharmacol Exp Ther **325,** 969, 2008.
19. Yao, L., Liu, J., and Andreadis, S.T. Composite fibrin scaffolds increase mechanical strength and preserve contractility of tissue engineered blood vessels. Pharm Res **25,** 1212, 2008.
20. Yao, L., Swartz, D.D., Gugino, S.F., Russell, J.A., and Andreadis, S.T. Fibrin-based tissue-engineered blood vessels: differential effects of biomaterial and culture parameters on mechanical strength and vascular reactivity. Tissue Eng **11,** 991, 2005.
21. Slaughter, B.V., Khurshid, S.S., Fisher, O.Z., Khademhosseini, A., and Peppas, N.A. Hydrogels in regenerative medicine. Adv Mater **21,** 3307, 2009.
22. Hoffman, M.P., Kibbey, M.C., Letterio, J.J., and Kleinman, H.K. Role of laminin-1 and TGF-beta 3 in acinar differentiation of a human submandibular gland cell line (HSG). J Cell Sci **109 (Pt 8),** 2013, 1996.
23. Joraku, A., Sullivan, C.A., Yoo, J., and Atala, A. *In-vitro* reconstitution of three-dimensional human salivary gland tissue structures. Differentiation **75,** 318, 2007.
24. Maria, O.M., Zeitouni, A., Gologan, O., and Tran, S.D. Matrigel improves functional properties of primary human salivary gland cells. Tissue Eng Part A **17,** 1229, 2011.
25. Swartz, D.D., Russell, J.A., and Andreadis, S.T. Engineering of fibrin-based functional and implantable small-diameter blood vessels. Am J Physiol Heart Circ Physiol **288,** H1451, 2005.
26. Turner, J.T., and Camden, J.M. The influence of vasoactive intestinal peptide receptors in dispersed acini from rat submandibular gland on cyclic AMP production and mucin release. Arch Oral Biol **35,** 103, 1990.
27. Quissell, D.O., Turner, J.T., and Redman, R.S. Development and characterization of immortalized rat parotid and submandibular acinar cell lines. Eur J Morphol **36 Suppl,** 50, 1998.
28. Turner, J.T., Redman, R.S., Camden, J.M., Landon, L.A., and Quissell, D.O. A rat parotid gland cell line, Par-C10, exhibits neurotransmitter-regulated transepithelial anion secretion. Am J Physiol **275,** C367, 1998.
29. Raut, S.D., Lei, P., Padmashali, R.M., and Andreadis, S.T. Fibrin-mediated lentivirus gene transfer: implications for lentivirus microarrays. J Control Release **144,** 213, 2010.
30. Baker, O.J., Camden, J.M., Redman, R.S., Jones, J.E., Seye, C.I., Erb, L., and Weisman, G.A. Proinflammatory cytokines tumor necrosis factor-alpha and interferon-gamma alter tight junction structure and function in the rat parotid gland Par-C10 cell line. Am J Physiol Cell Physiol **295,** C1191, 2008.
31. Jung, D.W., Hecht, D., Ho, S.W., O'Connell, B.C., Kleinman, H.K., and Hoffman, M.P. PKC and ERK1/2 regulate amylase promoter activity during differentiation of a salivary gland cell line. J Cell Physiol **185,** 215, 2000.
32. Lam, K., Zhang, L., Bewick, M., and Lafrenie, R.M. HSG cells differentiated by culture on extracellular matrix involves induction of S-adenosylmethione decarboxylase and ornithine decarboxylase. J Cell Physiol **203,** 353, 2005.
33. Maria, O.M., Maria, O., Liu, Y., Komarova, S.V., and Tran, SD. Matrigel improves functional properties of human submandibular salivary gland cell line. Int J Biochem Cell Biol **43,** 622, 2011.
34. Zheng, C., Hoffman, M.P., McMillan, T., Kleinman, H.K., and O'Connell, B.C. Growth factor regulation of the amylase promoter in a differentiating salivary acinar cell line. J Cell Physiol **177,** 628, 1998.
35. Ahmed, T.A., Dare, E.V., and Hincke, M. Fibrin: a versatile scaffold for tissue engineering applications. Tissue Eng Part B Rev **14,** 199, 2008.
36. Quissell, D.O., Barzen, K.A., Redman, R.S., Camden, J.M., and Turner, J.T. Development and characterization of SV40 immortalized rat parotid acinar cell lines. In Vitro Cell Dev Biol Anim **34,** 58, 1998.
37. Limesand, K.H., Barzen, K.A., Quissell, D.O., and Anderson, S.M. Synergistic suppression of apoptosis in salivary acinar cells by IGF1 and EGF. Cell Death Differ **10,** 345, 2003.
38. Redman, R.S., Quissell, D.O., and Barzen, K.A. Effects of dexamethasone, epidermal growth factor, and retinoic acid on rat submandibular acinar-intercalated duct complexes in primary culture. In Vitro Cell Dev Biol **24,** 734, 1988.
39. Redman, R.S. Myoepithelium of salivary glands. Microsc Res Tech **27,** 25, 1994.
40. Redman, R.S. On approaches to the functional restoration of salivary glands damaged by radiation therapy for head and neck cancer, with a review of related aspects of salivary gland morphology and development. Biotech Histochem **83,** 103, 2008.
41. Grundmann, O., Fillinger, J.L., Victory, K.R., Burd, R., and Limesand, K.H. Restoration of radiation therapy-induced salivary gland dysfunction in mice by post therapy IGF-1 administration. BMC Cancer **10,** 417, 2010.
42. Hand, A.R., Sivakumar, S., Barta, I., Ball, W.D., and Mirels, L. Immunocytochemical studies of cell differentiation during rat salivary gland development. Eur J Morphol **34,** 149, 1996.
43. Sivakumar, S., Mirels, L., Miranda, A.J., and Hand, A.R. Secretory protein expression patterns during rat parotid gland development. Anat Rec **252,** 485, 1998.
44. Quissell, D.O., Flaitz, C.M., Redman, R.S., and Barzen, K.A. Primary culture of human labial salivary gland acini. In Vitro Cell Dev Biol Anim **30A,** 736, 1994.
45. Yeh, C., Mertz, P.M., Oliver, C., Baum, B.J., and Kousvelari, E.E. Cellular characteristics of long-term cultured rat parotid acinar cells. In Vitro Cell Dev Biol **27A,** 707, 1991.
46. Zhang, Y., and Dong, C. Regulatory mechanisms of mitogen-activated kinase signaling. Cell Mol Life Sci **64,** 2771, 2007.
47. Patel, V.N., Rebustini, I.T., and Hoffman, M.P. Salivary gland branching morphogenesis. Differentiation **74,** 349, 2006.
48. Valentinis, B., Romano, G., Peruzzi, F., Morrione, A., Prisco, M., Soddu, S., Cristofanelli, B., Sacchi, A., and Baserga, R. Growth and differentiation signals by the insulin-like growth factor 1 receptor in hemopoietic cells are mediated through different pathways. J Biol Chem **274,** 12423, 1999.

49. Orton, R.J., Sturm, O.E., Vyshemirsky, V., Calder, M., Gilbert, D.R., and Kolch, W. Computational modelling of the receptor-tyrosine-kinase-activated MAPK pathway. Biochem J **392(Pt 2),** 249, 2005.
50. Peruzzi, F., Prisco, M., Dews, M., Salomoni, P., Grassilli, E., Romano, G., Calabretta, B., and Baserga, R. Multiple signaling pathways of the insulin-like growth factor 1 receptor in protection from apoptosis. Mol Cell Biol **19,** 7203, 1999.
51. Kashimata, M., Sayeed, S., Ka, A., Onetti-Muda, A., Sakagami, H., Faraggiana, T., and Gresik, E.W. The ERK-1/2 signaling pathway is involved in the stimulation of branching morphogenesis of fetal mouse submandibular glands by EGF. Dev Biol **220,** 183, 2000.
52. Kashimata, M.W., Sakagami, H.W., and Gresik, E.W. Intracellular signalling cascades activated by the EGF receptor and/or by integrins, with potential relevance for branching morphogenesis of the fetal mouse submandibular gland. Eur J Morphol **38,** 269, 2000.
53. Hayashi, T., Koyama, N., Gresik, E.W., and Kashimata, M. Detection of EGF-dependent microRNAs of the fetal mouse submandibular gland at embryonic day 13. J Med Invest **56 Suppl,** 250, 2009.
54. Koyama, N., Kashimata, M., Sakashita, H., Sakagami, H., and Gresik, E.W. EGF-stimulated signaling by means of PI3K, PLCgamma1, and PKC isozymes regulates branching morphogenesis of the fetal mouse submandibular gland. Dev Dyn **227,** 216, 2003.
55. van der Veeken, J., Oliveira, S., Schiffelers, R.M., Storm, G., van Bergen En Henegouwen, P.M., and Roovers, R.C. Crosstalk between epidermal growth factor receptor- and insulin-like growth factor-1 receptor signaling: implications for cancer therapy. Curr Cancer Drug Targets **9,** 748, 2009.
56. Hoffman, M.P., Kidder, B.L., Steinberg, Z.L., Lakhani, S., Ho, S., and Kleinman, H.K., Larsen, M. Gene expression profiles of mouse submandibular gland development: FGFR1 regulates branching morphogenesis *in vitro* through BMP- and FGF-dependent mechanisms. Development **129,** 5767, 2002.
57. Baggaley, E., McLarnon, S., Demeter, I., Varga, G., and Bruce, J.I. Differential regulation of the apical plasma membrane Ca(2+) -ATPase by protein kinase A in parotid acinar cells. J Biol Chem **282,** 37678, 2007.
58. Bockman, C.S., Bradley, M.E., Dang, H.K., Zeng, W., Scofield, M.A., and Dowd, F.J. Molecular and pharmacological characterization of muscarinic receptor subtypes in a rat parotid gland cell line: comparison with native parotid gland. J Pharmacol Exp Ther **297,** 718, 2001.
59. Rebustini, I.T., and Hoffman, M.P. ECM and FGF-dependent assay of embryonic SMG epithelial morphogenesis: investigating growth factor/matrix regulation of gene expression during submandibular gland development. Methods Mol Biol **522,** 319, 2009.
60. Nanduri, L.S., Maimets, M., Pringle, S.A., van der Zwaag, M., van Os, R.P., Coppes, R.P. Regeneration of irradiated salivary glands with stem cell marker expressing cells. Radiother Oncol **99**, 367, 2011.

Address correspondence to:
Olga J. Baker, DDS, PhD
Department of Oral Biology
School of Dental Medicine
University at Buffalo
The State University of New York
210 Foster Hall
Buffalo, NY 14214-3092

E-mail: olgabake@buffalo.edu

Received: November 15, 2012
Accepted: April 17, 2013
Online Publication Date: May 27, 2013